Heterogeneous interfacial chemical nature and bonds in a W-coated diamond/Al composite

Elsevier Editorial System(tm) for Materials Characterization

Manuscript Draft

Manuscript Number: MTL-15797R2

Title: Heterogeneous interfacial chemical nature and bonds in a W-coated diamond/Al composite

Article Type: Research paper

Keywords: Metal matrix composites (MMC); Scanning/transmission electron microscopy (STEM); Electron energy loss spectroscopy (EELS); Interface structure; Interfacial thermal resistance

Corresponding Author: Dr. gang ji, Ph.D.

Corresponding Author's Institution: Unité Matériaux et Transformations (UMET)

First Author: gang ji, Ph.D.

Order of Authors: gang ji, Ph.D.; Zhanqiu Tan, Ph.D.; Yinggang Lu, Ph.D.; Dominique Schryvers, Prof.; Zhiqiang Li, Prof.; Di Zhang, Prof.

Abstract: Heterogeneous Al/Al4C3/Al2O3/diamond{111}, Al/nanolayered Al4C3/diamond{111} and Al12W particle/Al4C3/Al2O3/diamond{111} multi-interfaces have been developed at the nanoscale in a W-coated diamond/Al composite produced by vacuum hot pressing. The formation of nanoscale Al4C3 crystals is strongly associated with local O enrichment and can be further promoted by Al12W interfacial particles. The latter effectively contributes to enhance interfacial chemical bonding reducing interfacial thermal resistance and, in turn, enhancing thermal conductivity.

Suggested Reviewers: Guosheng Shao
Institute for Renewable Energy and Environmental Technologies, University of Bolton

Paul Munroe
School of Materials Science and Engineering, University of New South Wales

He Tian
Center of Electron Microscopy, Department of Materials Science & Engineering,, Zhejiang University

Thomas Schubert
Department of Powder Metallurgy and Composite Materials, Fraunhofer-Institute for Manufacturing and Advanced Materials, Department of Powder Metallurgy and Composite Materials, Winterbergstr. 28, D-01277 Dresden, Germany

*Detailed Response to Reviewers

Dear Editor,

We would like to acknowledge again the reviewer No. 1 for his/her valuable and detailed comments. Based on the review reports, we improved our manuscript accordingly. The questions of the reviewer were answered below. All the modifications appeared in red color throughout the re-submitted manuscript:

Answer to the questions of reviewer No. 1:

Reviewer #1: The authors have reasonably well dealt with the comments of the reviewer. The reviewer still disagrees with the authors tentative to quantify the ITR via the AMM, but considers that this is a choice of the authors.

Question 1: A thing the reviewer didn't catch in the first reading is that the "tungsten-rich" particles are actually Al12W particles which raises the question where all the Tungsten coating has gone given that the diamond doesn't really look completely covered by those Al12W particles. At an initial coverage of 20-500 nm W-nanoparticles that should translate into easily a layer of 1 µm or more of the Al12W phase. Puzzling. If the authors have a good read on that it would be worthwhile explaining in the text.

Answer: Metallization of diamond particles by sol-gel process and additional heat treatment at 900 °C only introduces pure W nanoparticles but not W coating (see ref. [13]). In this work, we prepared several FIB samples of interface where only interfacial particles of $Al_{12}W$ have been indexed at the diamond/Al interface, and their size is comparable with that of initial W particles, in the range of 30-500 nm. The following sentence is revised to be more clear on this point "The deposited W ~~coating is discontinuous, and consists of~~ nanoparticles, with a size in the range 30-500 nm, ~~and~~ homogenously cover the surface of diamond particles".

Question 2: In the added text on p. 7: "being consistent" rather "being in consistence"

Answer: in the revised manuscript "being in consistence" has been replaced by "being consistent".

We look forward to your positive response.

Sincerely,

Gang JI

*Title Page

Heterogeneous interfacial chemical nature and bonds in a W-coated diamond/Al composite

Gang Ji [a,b,*], Zhanqiu Tan [c], Yinggang Lu [b,d], Dominique Schryvers [b], Zhiqiang Li [c,*], Di Zhang [c]

[a]*Unité Matériaux et Transformations, UMR CNRS 8207, Bâtiment C6, Université Lille 1, 59655 Villeneuve d'Ascq, France*
[b]*Electron Microscopy for Materials Science (EMAT), University of Antwerp, Groenenborgerlaan 171, 2020 Antwerp, Belgium*
[c]*State Key Laboratory of Metal Matrix Composites, Shanghai Jiao Tong University, Shanghai 200240, China*
[d]*Now at Department of Mechanical Engineering and Engineering Science, The University of North Carolina at Charlotte, Charlotte, NC 28223, USA.*

*Corresponding authors: Dr. G. JI; Prof. Z.Q. LI

	Dr. G. JI	Prof. Z.Q. LI
E-mail	gang.ji@univ-lille1.fr	lizhq@sjtu.edu.cn
Telephone number	+ 33 (0)320436965	+86 21138184173
Fax number	+ 33 (0)320436591	+ 86 2134202749

Abstract: Heterogeneous $Al/Al_4C_3/Al_2O_3/diamond_{\{111\}}$, Al/nanolayered $Al_4C_3/diamond_{\{111\}}$ and $Al_{12}W$ particle$/Al_4C_3/Al_2O_3/diamond_{\{111\}}$ multi-interfaces have been developed at the nanoscale in a W-coated diamond/Al composite produced by vacuum hot pressing. The formation of nanoscale Al_4C_3 crystals is strongly associated with local O enrichment and can be further promoted by $Al_{12}W$ interfacial particles. The latter effectively contributes to enhance interfacial chemical bonding reducing interfacial thermal resistance and, in turn, enhancing thermal conductivity.

Highlights:

(1) Heterogeneous multi-interfaces are developed in a W-coated diamond/Al composite.
(2) Formation of interfacial Al_4C_3 crystals is associated with local O enrichment.
(3) Presence of $Al_{12}W$ interfacial particles promotes interfacial chemical bonding.

Heterogeneous interfacial chemical nature and bonds in a W-coated diamond/Al composite

Gang Ji [a,b,*], Zhanqiu Tan [c], Yinggang Lu [b,d], Dominique Schryvers [b], Zhiqiang Li [c,*], Di Zhang [c]

[a]*Unité Matériaux et Transformations, UMR CNRS 8207, Bâtiment C6, Université Lille 1, 59655 Villeneuve d'Ascq, France*

[b]*Electron Microscopy for Materials Science (EMAT), University of Antwerp, Groenenborgerlaan 171, 2020 Antwerp, Belgium*

[c]*State Key Laboratory of Metal Matrix Composites, Shanghai Jiao Tong University, Shanghai 200240, China*

[d]*Now at Department of Mechanical Engineering and Engineering Science, The University of North Carolina at Charlotte, Charlotte, NC 28223, USA.*

*Corresponding authors: Dr. G. JI (gang.ji@univ-lille1.fr); Prof. Z.Q. LI (lizhq@sjtu.edu.cn)

Abstract: Heterogeneous Al/Al_4C_3/Al_2O_3/diamond$_{\{111\}}$, Al/nanolayered Al_4C_3/diamond$_{\{111\}}$ and $Al_{12}W$ particle/Al_4C_3/Al_2O_3/diamond$_{\{111\}}$ multi-interfaces have been developed at the nanoscale in a W-coated diamond/Al composite produced by vacuum hot pressing. The formation of nanoscale Al_4C_3 crystals is strongly associated with local O enrichment and can be further promoted by $Al_{12}W$ interfacial particles. The latter effectively contributes to enhance interfacial chemical bonding reducing interfacial thermal resistance and, in turn, enhancing thermal conductivity.

Keywords: Metal matrix composites (MMC); Scanning/transmission electron microscopy (STEM); Electron energy loss spectroscopy (EELS); Interface structure; Interfacial thermal resistance

1. Introduction

Basically, when a heat flux crosses a bi-material interface, a discontinuity developed in temperature distribution signals the existence of interfacial thermal resistance (ITR), also known as Kapitza resistance. ITR exists even at atomically perfect interfaces and low ITR is technologically important for applications where very high heat dissipation is necessary [1,2]. This is of particular concern to the development of advanced thermal management materials [3], like Al matrix composite reinforced with synthetic diamond particles (hereafter referred to as diamond/Al composite), in the microelectronic industry. However, in general, how interfacial chemistry and bonds affect ITR remains an open question [4].

In the diamond/Al composite, two priority issues should be considered to optimize ITR. On the one hand, it has been claimed that the formation of nanoscale Al_4C_3, due to the limited interfacial reaction between diamond and Al matrix, is beneficial for reducing ITR by improving interfacial bonding and, in turn, enhancing global thermal conductivity (TC); however, an excessive formation of Al_4C_3 degrades mechanical and thermal properties [5-7]. On the other hand, natural oxidation of as-received Al powder particles forming a nanosized Al_2O_3 skin [8] and possible oxygen gettering during following processing, like vacuum hot pressing (VHP), can introduce traces of oxygen at the diamond/Al interfacial area. Recent fundamental studies have shown that ITR can be significantly reduced with the increase of oxygen concentration at the diamond/Al interface by oxygenation of the diamond surface [9,10]. In contrast, at the Al/AlN interface the presence of an oxygen-rich interfacial layer of a few nanometers in thickness has been proven to be harmful for ITR [11]. In fact, both above-mentioned phenomena have simultaneously been involved in VHP processing of diamond/Al composites. However, their formation and combined effect on ITR at the nanoscale have been unclear so far.

Furthermore, analytical modelling has proposed that introduction of an additional W interfacial layer with a nanoscale thickness is one of the most beneficial ways for reducing ITR of the diamond/Al interface, since W has the highest TC among all the carbide-forming elements and very limited solubility in the Al matrix [12]. Experimentally, surface metallization of W on the surface of diamond particles has demonstrated its advantage in diamond/Al [13] as well as diamond/Cu composites [14] for global TC enhancement. However, the underlying mechanisms are still to be revealed since it seems that interfacial bonding is not the only key factor to determine ITR [15]. Hence, for the first time, we have used aberration-corrected high-resolution (scanning) transmission electron microscopy (HR(S)TEM) to investigate (heterogeneous) interfacial chemistry and bonds in a VHPed W-coated diamond/Al composite in order to develop our understanding of their complex effects on ITR at the nanoscale.

2. Material and Methods

In our previous work, W nanoparticles were deposited on the surface of diamond particles, having the average size of 200 μm, by a sol-gel approach; a W coated diamond/Al composite was produced by an optimized VHP process [13]. A nearly flat surface of the as-fabricated composite was acquired by triple ion beam cutting [16]. A FEI Helios NanoLab 650 dual beam system was used to prepare site-specific TEM samples for interfacial characterization. A FEI Tecnai G2 transmission electron microscope, operated at 200 kV, was used for (HR)TEM characterization. A state-of-the-art FEI "X-Ant-EM" microscope, equipped with a probe aberration corrector and a highly efficient (4 quadrant) energy dispersive X-ray (EDX) system and operated at 120 kV, was used for spatially resolved EDX and electron energy loss spectroscopy (EELS) mapping in the STEM mode. Convergent and collection semi-angles were set to around 21.5 and 37.0 mrad, respectively. The STEM/EELS was especially suitable

to map out the elemental distribution of interfacial oxygen, while the fine structure of the EELS edges (i.e., energy loss near edge structures (ELNES)) together with HRTEM provided easy access to phase identification at the nanoscale. Precession electron diffraction (PED) was performed by using a Philips CM20 microscope, operated at 200 kV and equipped with a Nanomegas 'Spinning Star' precession unit. The precession semi-angle of 2° was set to record a PED zone-axis pattern (ZAP), which significantly reduced the overall dynamical effects. JEMS software was used for simulation of ZAPs by considering the kinematical approximation.

3. Results and Discussion

The deposited W ~~coating is discontinuous, and consists of~~ nanoparticles, with a size in the range 30-500 nm, ~~and~~ homogenously cover the surface of diamond particles [13]. The TC of the VHPed W-coated diamond (50 vol.%) /Al composite is as high as around 600 W/m K, which is about 20 % higher than that (496 W/m K) of the composite without such a coating [13]. Fig. 1a is an overview of the diamond$_{\{111\}}$/Al interface where a W-rich particle of several hundred nanometers in size can be identified by TEM/EDX analysis (Fig. 1b). A close look (Fig. 1c) reveals that this W-rich particle, corresponding to the $Al_{12}W$ phase, consists of two parts. Fine particle-like features are also visible to be located at the particle/particle and particle/diamond interfaces where the concentrations of O are correspondingly high (Fig. 1d). Again in Fig. 1c, three characteristic interfacial areas in the boxes Nos. 1, 2 and 3 are selected for further characterization in the STEM mode.

As shown in Figs. 2a and 3a, the interfaces in the boxes Nos. 1 and 2 are next to each side of the W-rich particle contained interfacial area, respectively. However, they present completely different fine microstructure. In the box No. 1 (Fig. 2a), the plate-like Al_4C_3, having a length of around 90 nm and a width of 15 nm (i.e. the aspect ratio of 6), tightly lays

upon the {111} face of diamond where, in between, a thin α-Al_2O_3 layer of around 1.5 nm in thickness estimated from the HRTEM image (Fig. 2c) is present. The measured ELNES of the relevant ionization edges (Al L_{23}-edge and C K-edge) are plotted in Figs. 2b and 2d, and compared with those of standard pure Al, α-Al_2O_3 and Al_4C_3 [17,18] and diamond [19]. The different Al compounds and diamond have been identified by mainly considering the edge onset, the shape and the energy position featured in each ELNES. In Fig. 2b, the Al L_{23}-edge fine structure of pure Al matrix next to the diamond$_{\{111\}}$/Al interface starts at around 72.5 eV with a broad peak at 98.5 eV, while that of α-Al_2O_3 displays three peaks at around 80, 85 and 99.5 eV with the onset energy of 75 eV. The Al L_{23}-edge ELNES of Al_4C_3 is distinctly different from those of pure Al and α-Al_2O_3, and displays two peaks at around 78 and 98.5 eV. In Fig. 2d, the onset energies of the C k-edge fine structure are around 282 eV for Al_4C_3 and 288 eV for diamond, which are accompanied by the peaks centered at 291 and 305 eV for Al_4C_3 and 292, 298 and 305.5 eV for diamond. Hence, an Al/Al_4C_3/Al_2O_3/diamond$_{\{111\}}$ multi-interface is clearly revealed by STEM/EELS together with HRTEM. Comparatively, a 'clean' interface without the trace of interfacial O (i.e., Al_2O_3) is revealed in the box No. 2 (Fig. 3). Instead, a thin interfacial Al_4C_3 layer of around 2 nm in thickness is found. The Al L_{23}-edge ELNES of pure Al and Al_4C_3 plotted in Fig. 3b are very similar to those from the box No. 1 (Fig. 2b). In this case, an Al/nanolayered Al_4C_3/diamond$_{\{111\}}$ multi-interface is developed. In the same way at the W-rich particle/diamond interfacial area (Fig. 4), an $Al_{12}W$ particle/Al_4C_3/Al_2O_3/diamond$_{\{111\}}$ multi-interface is characterized. In summary, at the nanoscale the three typical interfacial configurations at the W-coated diamond/Al interface are: Al/Al_4C_3/Al_2O_3/diamond$_{\{111\}}$, Al/nanolayered Al_4C_3/diamond$_{\{111\}}$ and $Al_{12}W$ particle/Al_4C_3/Al_2O_3/diamond$_{\{111\}}$ multi-interfaces. The results also indicate that the development of Al_4C_3, from an initial nanolayered structure (Fig. 3) to perfect crystals (Figs.

2 and 4), is strongly associated with the presence of interfacial O. In addition, the formation of the nanoscale Al_4C_3 is promoted in the $Al_{12}W$ particle contained interfacial area (Fig. 1c).

As plotted in Fig. 3d, the derived average ITR of the W-coated composite (0.13×10^{-7} m^2 K/W) is around three times lower than that of the uncoated one (0.43×10^{-7} m^2 K/W), which shows unequivocal benefit of the interfacial $Al_{12}W$ particles for reducing the ITR. As shown by the inset of Fig. 3d, the characterized heterogeneous bonds in Figs 2, 3 and 4 can be approximate to the Al/Al_4C_3/diamond, 'clean' (diffusion-bonded) Al/diamond and $Al/Al_{12}W$/diamond interfaces, respectively. In general, ITR increases with each additional layer introduced at the interface and its thickness by considering an electrical resistance analogy and using the AMM [12]. From this point of view, the 'clean' diamond/Al interface (Fig. 3) is the most favourable in order to minimize ITR by facilitating transmission of phonons across the interface, with the calculated ITR of around 0.22×10^{-7} m^2 K/W [12]. Provided that the 'clean' and Al/Al_4C_3/diamond interfaces are both involved in the uncoated composite, the ITR of the Al/Al_4C_3/diamond interface is deduced to be in the range 0.22-0.43×10^{-7} m^2 K/W. As long as the specific heat (618.6 J/kg K) of $Al_{12}W$ is estimated by the rule of mixtures, and using the density (3880 kg/m^3) of $Al_{12}W$ from PDF#65-1786 and the sound velocity (4155 m/s) of $Al_{12}W$ from ref. [20], the ITR of the $Al/Al_{12}W$ (500 nm in thickness)/diamond interface is calculated to be 0.13×10^{-7} m^2 K/W by the AMM and assuming the TC (230 W/m K) of $Al_{12}W$ the same as that of pure Al. Hence, the calculation results suggest that the contribution of the interfacial $Al_{12}W$ particles may be compensated by the promotion of interfacial bonding to bring the average ITR down to 0.13×10^{-7} m^2 K/W in the W-coated composite. If the TC of $Al_{12}W$ is assumed to be much lower than pure Al, this compensation should be more pronounced due to the higher ITR of $Al_{12}W$ (e.g., 0.21×10^{-7} m^2 K/W for the TC of 50 W/m K).

It has been documented that the reactivity of the {100} face of diamond with Al in the solid state [13] and liquid Al [21] is higher than that of the {111} face, which has a significant impact on interfacial bonding strength and ITR. In fact, compared with the three-fold bonded C atoms of the {111} surfaces of diamond, the two-fold bonded C atoms of the {100} surfaces are more easily to be liberated to form Al_4C_3 [21]. Formation of the interfacial $Al_{12}W$ particles, due to reaction sintering during the VHP process and the low solubility of W in Al (e.g., 0.024 at.% at 660 °C [12]), reduces such a reactivity difference of the diamond faces and significantly promotes the formation of nanoscale Al_4C_3 at the diamond$_{\{111\}}$/Al interface, as evidenced in Fig. 1c. Examinations of fracture surface also confirm that both {100} and {111} surfaces of diamond in the W-coated diamond/Al composite show good bonding with the Al matrix [13]. Hence, experimental evidences reveal that diamond surface metallization by deposition of W nanoparticles definitively enhances interfacial bonding state of the {111} surface of diamond which contributes to the improved TC, being consistent with the above-mentioned calculations. Furthermore, only the nanosized W particles rather than a continuous W layer are deposited at the surface of diamond particles. As a result, the uncovered diamond surface can also be affected by the sol-gel and additional heat treatments (at 900 °C for 30 min and in the 20%H_2-Ar atmosphere [13]). It has been reported that hydrogenation and acid treatment of diamond can change its surface chemistry to have a significant impact on ITR [9,10].

Interestingly, there is always a close link between the development of Al_4C_3 and local O enrichment at the diamond/Al interface. The nucleation of Al_4C_3 at the surface of diamond particles needs the flash surface of pure Al which can be properly provided by local breakdown of the initial Al_2O_3 skin during the VHP process. The nanosized Al_2O_3 segments (or agglomerations) accumulated surrounding the interface at the side of the Al matrix can introduce local lattice distortion associated with dislocation pinning, which may accelerate the

diffusion of C atoms to promote precipitation reaction of the interfacial Al_4C_3 crystals. It has been found in cast graphite/Al composites that the morphology of interfacial Al_4C_3 strongly depends on processing conditions; the diffuse interface migrates much faster than the flat one to have a large aspect ratio under a low growth driving force (e.g., at the low melting temperature) [22]. Comparatively, as revealed in the boxes 1 (Fig. 2), 2 (Fig. 3) and 3 (Fig. 4), the different morphology of nanoscale Al_4C_3 has been developed at the diamond/Al interface but in the same sample. The higher aspect ratio of the interfacial Al_4C_3 crystal in the Al matrix (Fig. 2) when compared with that of the $Al_{12}W$ particle (Fig. 4) suggests a more rapid diffusion rate of C atoms in Al than in $Al_{12}W$. At the uncovered diamond surface, the different morphology of Al_4C_3 (Figs. 2 and 3) may originate from local surface state of diamond due probably to initial surface metallization and random distribution of Al_2O_3 particles in the Al matrix, which delicately modify nucleation and growth mechanisms of local Al_4C_3 from one interfacial area to another at the nanoscale. Such microstructural features also provide a hint that process optimization alone is unavailable to acquire a homogenous diffusion-bonded interface (the case in Fig. 3) in the diamond/Al composite, although it is regarded as the ideal interface for minimizing ITR as proposed in [1,7,12]. Further, the orientation relationship between diamond particles and Al_4C_3 in pressure infiltrated diamond/Al composites has recently been determined to be $[1\bar{1}0]_{diamond}//[100]_{Al4C3}$ and $(111)_{diamond}//(003)_{Al4C3}$ on both {111} and {100} diamond surfaces [23]. Such an orientation relationship may exist in both interfaces in our case (Figs. 2 and 3) since the measured spacing of $(0012)_{Al4C3}$ planes (d=0.208 nm), being parallel to $(111)_{diamond}$, is exactly four times smaller than that of $(003)_{Al4C3}$ planes (d=0.832 nm).

Finally, it should be mentioned that a quantitative correlation of the above mentioned interfacial bonds at the nanoscale, presented by the newly formed compounds, with the theoretical ITR is still impossible at this stage for the following reasons. First, to the best

knowledge of the authors, directly measured physical properties (e.g., sound velocity or TC) of the Al_4C_3 and $Al_{12}W$ are unavailable in the literature, which impedes the ITR of each bond to be calculated by using an acoustic mismatch model (AMM) [12]. Second, the content of each bond in the composite cannot be easily obtained so that the average ITR cannot be estimated. Third, the AMM assumes a perfect and strong bond at the interface, while a recently proposed (modified) model takes into account the effect of weak bonding by introducing adhesion energy, and indicates that the ITR difference between weak and strong bonds can be as high as one order of magnitude [24].

4. Summary and conclusions

The nanoscale Al/Al_4C_3/Al_2O_3/diamond$_{\{111\}}$, Al/nanolayered Al_4C_3/diamond$_{\{111\}}$ and $Al_{12}W$ particle/Al_4C_3/Al_2O_3/diamond$_{\{111\}}$ multi-interfaces developed in the W-coated diamond/Al composite have successfully been characterized by HR(S)TEM. The $Al_{12}W$ particle/Al_4C_3/Al_2O_3/diamond$_{\{111\}}$ multi-interfaces contribute to increase local bonding strength by reducing the reactivity difference between the {111} and {100} diamond faces promoting the formation of Al_4C_3 at the diamond$_{\{111\}}$/Al interface. As a result, such heterogeneous interfacial chemical bonds are beneficial for TC improvement compared with the uncoated composite counterpart. However, the quantitative relationship between the interfacial bonding strength, nature of interfacial bonds and ITR still remains unclear. The physical properties of Al_4C_3 and $Al_{12}W$ should be established to develop a sophisticated AMM calculation to fully describe the experimental evidence at the nanoscale.

Acknowledgments

This work is financially supported by the FWO project of Belgium (No. U2 FA 070100/3506), the travel funding BQR (No. R8DIV AUE) provided by Université Lille 1, the National Natural Science Foundation of China (Grant No. 51401123) and the China

Postdoctoral Science Foundation (Grant No. 2014M561469) for Dr. Z.Q. Tan. Dr. W.G. Grünewald (Leica Microsystems, Germany) is also thanked for the assistance of surface preparation.

References

[1] T. Schubert, Ł. Ciupiński, W. Zieliński, A. Michalski, T. Weißgärber, B. Kieback, Interfacial characterization of Cu/diamond composites prepared by powder metallurgy for heat sink applications, Scr. Mater. 58 (2008), pp. 263-266

[2] C. Monachon, L. Weber, Thermal boundary conductance between refractory metal carbides and diamond, Acta Mater. 73 (2014), pp. 337-346

[3] A. Luedtke, Thermal Management Materials for High-Performance Applications, Adv. Eng. Mater. 6 (2004), pp. 142-144

[4] M.D. Losego, D.G. Cahill, Thermal transport: Breaking through barriers, Nature mater. 12 (2013), pp. 382-384

[5] W.B. Johnson, B. Sonuparlak, Diamond/Al metal matrix composites formed by the pressureless metal infiltration process, J. Mater. Res. 8 (1993), pp. 1169-1173

[6] P.W. Ruch, O. Beffort, S. Kleiner, L. Weber, P.J. Uggowitzer, Selective interfacial bonding in Al(Si)–diamond composites and its effect on thermal conductivity, Compos. Sci. Technol. 66 (2006), pp. 2677-2685

[7] I.E. Monje, E. Louis, J.M. Molina, Optimizing thermal conductivity in gas-pressure infiltrated aluminum/diamond composites by precise processing control, Compos. part A 48 (2013), pp. 9-14

[8] L. Jiang, Z.Q. Li, G.L. Fan, D. Zhang, A flake powder metallurgy approach to Al_2O_3/Al biomimetic nanolaminated composites with enhanced ductility, Scr. Mater. 65 (2011), pp. 412-415

[9] K.C. Collins, S. Chen, G. Chen, Effects of surface chemistry on thermal conductance at aluminum–diamond interfaces, Appl. Phys. Lett. 97 (2010), pp. 083102

[10] C. Monachon, L. Weber, Influence of diamond surface termination on thermal boundary conductance between Al and diamond, J. Appl. Phys. 113 (2013), pp. 183504

[11] C. Monachon, M. Hojeij, L. Weber, Influence of sample processing parameters on thermal boundary conductance value in an Al/AlN system, Appl. Phys. Lett. 98 (2011), pp. 091905

[12] Z.Q. Tan, Z.Q. Li, D.B. Xiong, G.L. Fan, G. Ji, D. Zhang, A predictive model for interfacial thermal conductance in surface metallized diamond aluminum matrix composites, Mater. Design 55 (2014), pp. 257-262

[13] Z.Q. Tan, Z.Q. Li, G.L. Fan, Q. Guo, X.Z. Kai, G. Ji, L.T. Zhang, D. Zhang, Enhanced thermal conductivity in diamond/aluminum composites with a tungsten interface nanolayer, Mater. Design 47 (2013), pp. 160-166

[14] A.M. Abyzov, S.V. Kidalov, F.M. Shakhov, High thermal conductivity composites consisting of diamond filler with tungsten coating and copper (silver) matrix, J. Mater. Sci. 46 (2011), pp. 1424-1438

[15] A.M. Abyzov, M.J. Kruszewski, Ł. Ciupiński, M. Mazurkiewicz, A. Michalski, K.J. Kurzydłowski, Diamond–tungsten based coating–copper composites with high thermal conductivity produced by Pulse Plasma Sintering, Mater. Design 76 (2015), pp. 97-109

[16] G. Ji, Z.Q. Tan, R. Shabadi, Z.Q. Li, W.G. Grünewald, A. Addad, D. Schryvers, D. Zhang, Triple ion beam cutting of diamond/Al composites for interface characterization, Mater. Charact. 89 (2014), pp. 132-137

[17] A. Feldhoff, E. Pippel, J. Woltersdorf, Structure and composition of ternary carbides in carbonfibre reinforced Mg-Al alloys, Phil. Mag. A 79 (1999), pp. 1263-1277

[18] I. Levin, A. Berner, C. Scheu, H. Muellejans, D.G. Brandon, Electron Energy-Loss Near-Edge Structure of Alumina Polymorphs, Mikrochim. Acta [Suppl.] 15 (1998), pp. 93-96

[19] Y.G. Lu, S. Turner, J. Verbeeck, S.D. Janssens, P. Wagner, K. Haenen, G.V. Tendeloo, Direct visualization of boron dopant distribution and coordination in individual chemical vapor deposition nanocrystalline B-doped diamond grains, Appl. Phys. Lett. 101 (2012), pp. 041907

[20] X.M. Tao, Y.Z. Liu, R.H. Wang, Y.F. Ouyang, Y. Du, Y.H. He, First-principles investigations of elastic, electronic and thermodynamic properties of $Al_{12}X$ (X = Mo, W and Re), Intermetallics 24 (2012), pp. 15-21

[21] S. Kleiner, F.A. Khalid, P.W. Ruch, S. Meier, O. Beffort, Effect of diamond crystallographic orientation on dissolution and carbide formation in contact with liquid aluminium, Scr. Mater. 55 (2006), pp. 291-294

[22] H.N. Yang, M.Y. Gu, W.J. Jiang, G.D. Zhang, Interface microstructure and reaction in Gr/Al metal matrix composites, J. Mater. Sci. 31 (1996), pp. 1903

[23] Z.F. Che, Y. Zhang, J.W. Li, H.L. Zhang, X.T. Wang, C. Sun, J.G. Wang, M.J. Kim, Nucleation and growth mechanisms of interfacial Al_4C_3 in Al/diamond composites, J. Alloys Comp. 657 (2016), pp. 81-89

[24] R. Prasher, Acoustic mismatch model for thermal contact resistance of van der Waals contacts, Appl. Phys. Lett. 94 (2009), pp. 041905

Figure captions

Figure 1. (a) TEM bright-field (BF) image showing the diamond$_{\{111\}}$/Al interface in the as-prepared FIB sample; (b) EDX spectrum of the W-rich interfacial particle double arrowed in (a); (c) STEM/ADF image highlighting the particle-contained interfacial area and (d) corresponding mixed O (red), Al (dark blue), W (clear blue) and C (green) STEM/EDX map (after background subtraction). Inset in (a) is the [011] ZAP of diamond with adjusted orientation relationship with respect to image and inset in (c) is the [111] PED ZAP of the doubled arrowed particle corresponding to $Al_{12}W$ phase. Note that interfacial areas in boxes namely Nos. 1, 2 and 3 in (c) are selected for further analyses.

Figure 2. (a) TEM BF image highlighting the interfacial area in the box No. 1 shown in Fig. 1c containing, from top to bottom, Al matrix, Al_4C_3, Al_2O_3 and diamond; (b) and (d) corresponding Al L-edge and C k-edge fine structures; respectively and (c) HRTEM image of the Al_4C_3/Al_2O_3/diamond interface in the box in (a). Insets in (a) is the O map showing the trace of interfacial O, while that in (c) is the corresponding [011] FFT pattern of diamond.

Figure 3. (a) TEM BF image highlighting the interfacial area in the box No. 2 shown in Fig. 1c containing, from top to bottom, Al matrix, Al_4C_3 and diamond; (b) corresponding Al L-edge fine structure and (c) HRTEM image of the Al matrix/Al_4C_3/diamond interface in the box in (a). Inset in (a) is the O map without the trace of interfacial O, while that in (c) is the corresponding [011] FFT pattern of diamond. (d) Average ITR values derived from the measured TCs of the W-coated and uncoated diamond/Al composites in terms of differential effective medium (DEM) scheme, inset is the schematic of simplified heterogeneous interfacial configurations in the W-coated composite.

Figure 4. (a) TEM BF image highlighting the interfacial area in the box No. 3 shown in Fig. 1c containing, from top to bottom, W-rich particle, Al_4C_3, Al_2O_3 and diamond; (b) corresponding C k-edge fine structure. Inset in (a) is the O map with the trace of interfacial O.

Figure 1

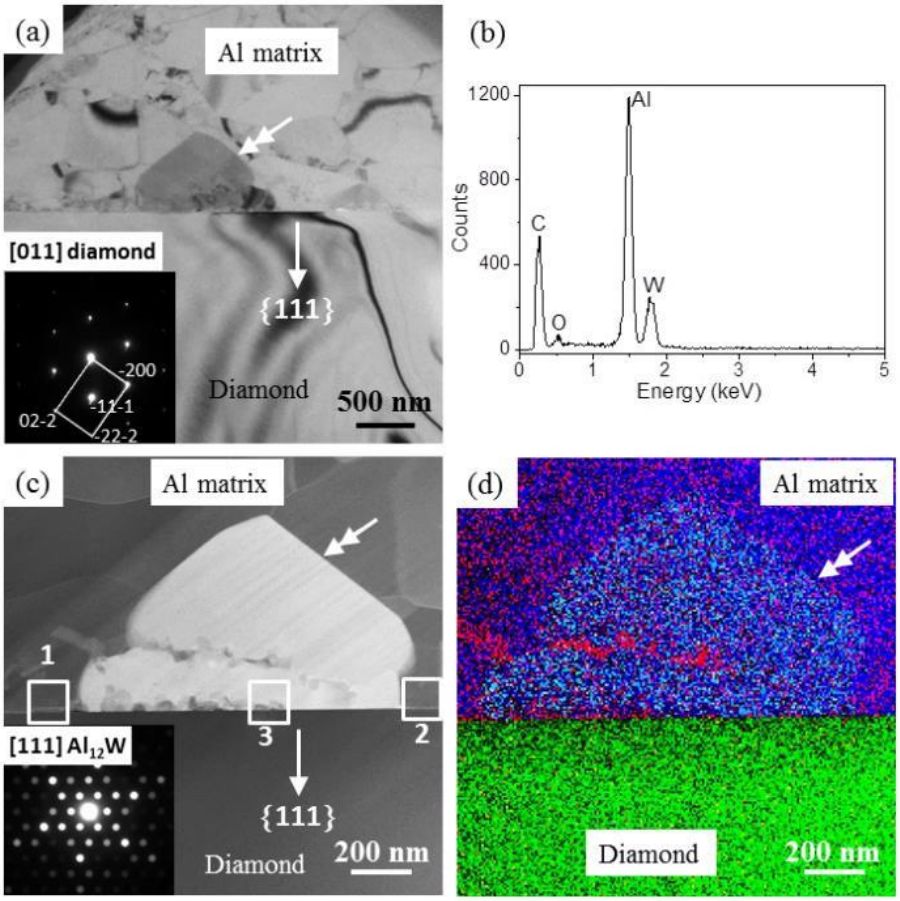
(a)
Al matrix
[011] diamond
-200
-11-1
02-2
-22-2
{111}
Diamond
500 nm
(b)
Al
C
O
W
Counts
Energy (keV)
(c)
Al matrix
1
2
3
[111] Al12W
{111}
Diamond
200 nm
(d)
Al matrix
Diamond
200 nm

Figure 2

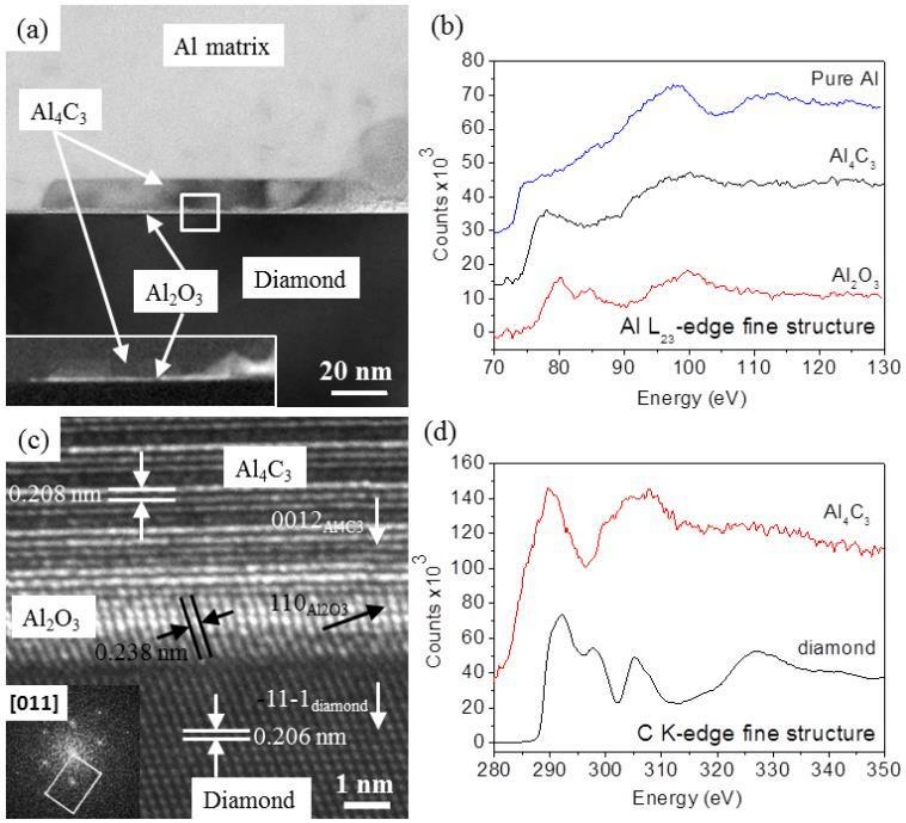
(a)
Al matrix
Al_4C_3
Al_2O_3
Diamond
20 nm
(b)
Pure Al
Al_4C_3
Al_2O_3
Al L_{23}-edge fine structure
Counts x10^3
Energy (eV)
(c)
Al_4C_3
0.208 nm
0012_{Al4C3}
Al_2O_3
110_{Al2O3}
0.238 nm
[011]
$-11-1_{diamond}$
0.206 nm
Diamond
1 nm
(d)
Al_4C_3
diamond
C K-edge fine structure
Counts x10^3
Energy (eV)

Figure 3

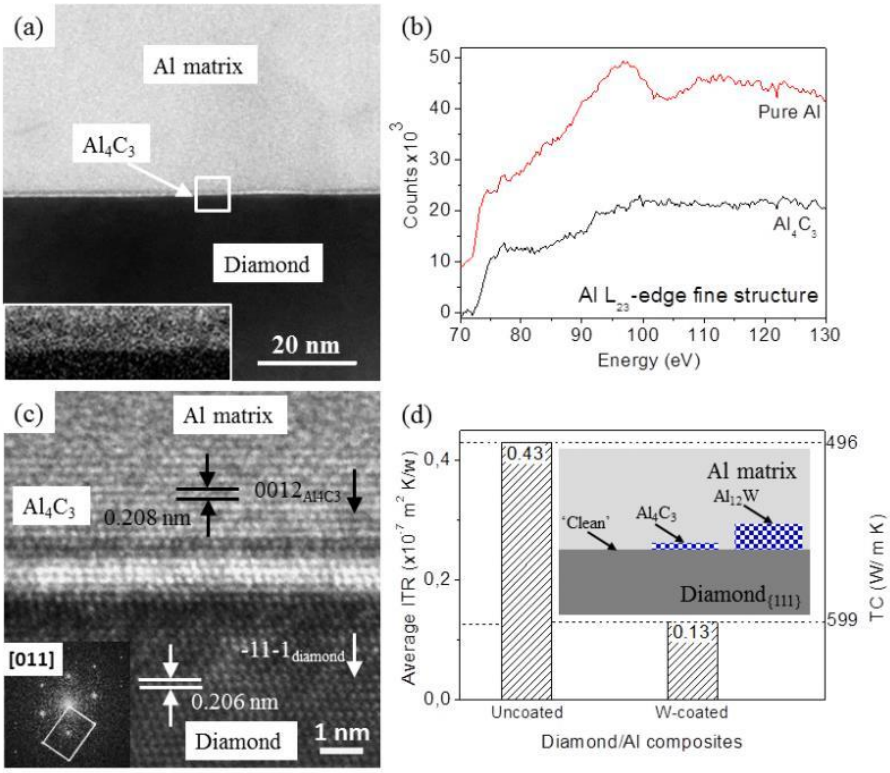
(a)
Al matrix
Al_4C_3
Diamond
20 nm
(b)
Counts x10^3
Pure Al
Al_4C_3
Al L_{23}-edge fine structure
Energy (eV)
(c)
Al matrix
Al_4C_3
0.208 nm
0012_{Al4C3}
[011]
$-11-1_{diamond}$
0.206 nm
Diamond
1 nm
(d)
Average ITR (x10^{-7} m^2 K/W)
0.43
0.13
Al matrix
$Al_{12}W$
'Clean'
Al_4C_3
$Diamond_{\{111\}}$
496
599
TC (W/ m K)
Uncoated
W-coated
Diamond/Al composites

Figure 4

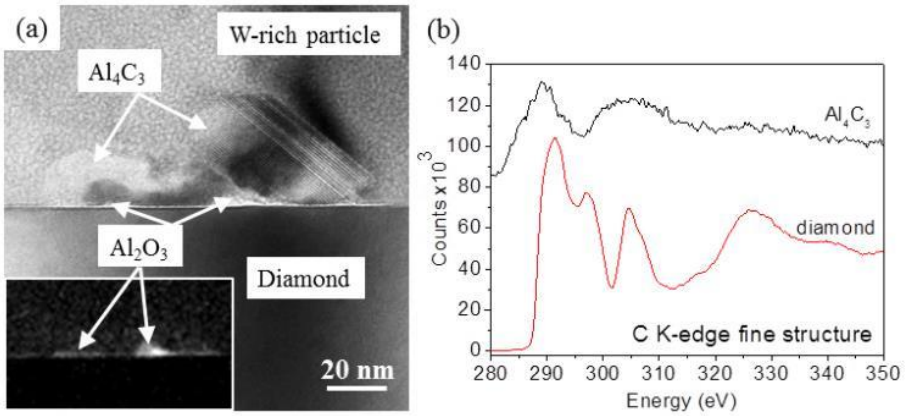
(a)
W-rich particle
Al_4C_3
Al_2O_3
Diamond
20 nm
(b)
Al_4C_3
diamond
C K-edge fine structure
Counts x10^3
Energy (eV)
0
20
40
60
80
100
120
140
280
290
300
310
320
330
340
350